# A Joint Probabilistic Model for Speckle Variance, Amplitude Decorrelation and Interframe Variance (IFV) Optical Coherence Tomography Angiography

Stefan B. Ploner[1], Christian Riess[1], Julia Schottenhamml[1,2], Eric M. Moult[2], Nadia K. Waheed[3], James G. Fujimoto[2], Andreas Maier[1]

[1]Pattern Recognition Lab, FAU Erlangen-Nürnberg, Germany
[2]Department of Electrical Engineering and Computer Science, Research Laboratory for Electronics, Massachusetts Institute of Technology, Cambridge, MA, USA
[3]Ophthalmology, New England Eye Center, Tufts Medical Center, Boston, MA, USA
stefan.ploner@fau.de

**Abstract.** Optical Coherence Tomography Angiography (OCTA) is a general method to visualize blood flow in biological tissue. Despite its good results in practice, the commonly used Amplitude Decorrelation OCTA (AD-OCTA) measure suffers from a well-understood objective function, which makes it challenging to mathematically model post processing tasks like, e.g., denoising.
In this paper, a probabilistic model is developed for the three OCTA measures Speckle Variance OCTA, AD-OCTA and the newly proposed Interframe Variance OCTA (IFV-OCTA) to enable further tasks like regularization-based denoising. From a theoretical point of view, IFV-OCTA is shown to be in-between the other two methods and can act as a link between them. A small sized observer study suggests that the image quality of IFV-OCTA is comparable to the other methods. IFV-OCTA is a promising OCTA measure for algorithms that require a dependency on the interscan time.

## 1 Introduction

Optical Coherence Tomography (OCT) is a 3D imaging modality based on low coherence interferometry that achieves micron-scale resolution in biological tissue [1]. Its fast acquisition speed, up to real time imaging, and the non-invasiveness led to its adaption in many clinical fields, in particular in ophthalmology. By analyzing the differences of repeated scans, an angiographic signal can be formed, which is called OCT angiography (OCTA). In contrast to doppler techniques, which are based on the signal's phase information, the herein compared OCTA measures are only dependent on the signal intensity.

In this work, a common probabilistic model is developed for three different OCTA measures, which are Speckle Variance OCTA (SV-OCTA) [2], Amplitude Decorrelation OCTA (AD-OCTA) [3] and a newly proposed method.

Whereas SV-OCTA has, as the name tells, a clear probabilistic interpretation, namely the variance of the signal, such an interpretation was missing for AD-OCTA. We derived a probabilistic model, whose solution is equivalent to the AD-OCTA method. We further introduce the Interframe Variance OCTA (IFV-OCTA) method, which acts as a link between SV-OCTA and AD-OCTA.

Finally, we compared the image quality of the three methods in an observer study, which was performed on the full 3D volume. Five different cases were analyzed by five expert graders.

## 2 Materials and Methods

First, the probabilistic model for the three OCTA measures is introduced. Then, the details of the observer study are described.

### 2.1 Probabilistic Models

For each OCTA measure, an objective function $L$ is formulated based on the voxel intensities $a_i, i \in 1, \ldots, N$, where $N$ is the number of repeated B-scans per location in the OCT scan protocol and $\mu = \frac{1}{N}\sum_{i=1}^{N} a_i$ is the mean of the intensities.

**Speckle variance OCTA (SV-OCTA)** The SV-OCTA method has a probabilistic interpretation, which is the variance of the repeatedly acquired samples. This can easily be shown with a standard maximum likelihood estimation of the parameters $\mu$ and $\sigma_{\mathrm{SV}}^2$, by assuming normally distributed $a_i$ in the objective function $L_{\mathrm{SV}}$.

$$L_{\mathrm{SV}} = \prod_{i=1}^{N} \mathrm{p}\left(a_i \,|\, \mu, \sigma_{\mathrm{SV}}^2\right) = \prod_{i=1}^{N} \frac{1}{\sqrt{2\pi\sigma_{\mathrm{SV}}^2}} \exp\left(-\frac{(a_i-\mu)^2}{2\sigma_{\mathrm{SV}}^2}\right) \tag{1}$$

$$\max_{\mu,\sigma_{\mathrm{SV}}^2}\left\{L_{\mathrm{SV}}\right\} = \max_{\mu,\sigma_{\mathrm{SV}}^2}\left\{\log L_{\mathrm{SV}}\right\} = \max_{\mu,\sigma_{\mathrm{SV}}^2}\left\{N \cdot \log \frac{1}{\sqrt{2\pi\sigma_{\mathrm{SV}}^2}} - \sum_{i=1}^{N} \frac{(a_i-\mu)^2}{2\sigma_{\mathrm{SV}}^2}\right\} \tag{2}$$

We then locate the $\sigma_{\mathrm{SV}}^2$ that produces the measured data with highest probability by setting the respective derivative to zero.

$$\frac{d \log L_{\mathrm{SV}}}{d\sigma_{\mathrm{SV}}^2} = \frac{-N \cdot \sigma_{\mathrm{SV}}^2 + \sum_{i=1}^{N}(a_i-\mu)^2}{2\sigma_{\mathrm{SV}}^4} \overset{!}{=} 0 \tag{3}$$

$$\sigma_{\mathrm{SV}}^2 = \frac{1}{N}\sum_{i=1}^{N}(a_i-\mu)^2 \tag{4}$$

**Interframe Variance (IFV-OCTA)** The newly proposed Interframe Variance measure is the variance of the differences of the voxel intensities. Note that the mean value of these differences is zero due to the identical distribution of the values. Again, by setting the derivative of the new objective function $L_{\text{IFV}}$ to zero, a direct computation formula can be derived, which is denoted in Eq. (8).

$$L_{\text{IFV}} = \prod_{i=1}^{N-1} \text{p}\left(a_i - a_{i+1} \,|\, 0, \sigma^2_{\text{IFV}}\right) = \prod_{i=1}^{N-1} \frac{1}{\sqrt{2\pi\sigma^2_{\text{IFV}}}} \exp\left(-\frac{(a_i - a_{i+1})^2}{2\sigma^2_{\text{IFV}}}\right) \tag{5}$$

$$\log L_{\text{IFV}} = (N-1) \cdot \log \frac{1}{\sqrt{2\pi\sigma^2_{\text{IFV}}}} - \sum_{i=1}^{N-1} \frac{(a_i - a_{i+1})^2}{2\sigma^2_{\text{IFV}}} \tag{6}$$

$$\frac{d \log L_{\text{IFV}}}{d\sigma^2_{\text{IFV}}} = \frac{-(N-1) \cdot \sigma^2_{\text{IFV}} + \sum_{i=1}^{N-1} (a_i - a_{i+1})^2}{2\sigma^4_{\text{IFV}}} \stackrel{!}{=} 0 \tag{7}$$

$$\sigma^2_{\text{IFV}} = \frac{1}{N-1} \sum_{i=1}^{N-1} (a_i - a_{i+1})^2 \tag{8}$$

**Amplitude Decorrelation (AD-OCTA)** The AD-OCTA method is defined by its direct computation formula [3]. Thus, this time we set up an objective function $L_{\text{AD}}$ which yields a $\sigma^2_{\text{AD}}$ that matches the AD-OCTA computation formula. Similar to IFV-OCTA, the objective function is based on the difference between consecutive voxel intensities. However, for AD-OCTA, the difference is normalized by its amplitude through a multiplication with the factor $\frac{1}{\sqrt{a_i^2 + a_{i+1}^2}}$.

$$L_{\text{AD}} = \prod_{i=1}^{N-1} \text{p}\left(\frac{a_i}{\sqrt{a_i^2 + a_{i+1}^2}} - \frac{a_{i+1}}{\sqrt{a_i^2 + a_{i+1}^2}} \,|\, 0, \sigma^2_{\text{AD}}\right) \tag{9}$$

$$= \prod_{i=1}^{N-1} \frac{1}{\sqrt{2\pi\sigma^2_{\text{AD}}}} \exp\left(-\frac{\frac{(a_i - a_{i+1})^2}{a_i^2 + a_{i+1}^2}}{2\sigma^2_{\text{AD}}}\right) \tag{10}$$

$$\log L_{\text{AD}} = (N-1) \cdot \log \frac{1}{\sqrt{2\pi\sigma^2_{\text{AD}}}} - \sum_{i=1}^{N-1} \frac{\frac{(a_i - a_{i+1})^2}{a_i^2 + a_{i+1}^2}}{2\sigma^2_{\text{AD}}} \tag{11}$$

$$\frac{d \log L_{\text{AD}}}{d\sigma^2_{\text{AD}}} = \frac{-(N-1) \cdot \sigma^2_{\text{AD}} + \sum_{i=1}^{N-1} \frac{(a_i - a_{i+1})^2}{a_i^2 + a_{i+1}^2}}{2\sigma^4_{\text{AD}}} \stackrel{!}{=} 0 \tag{12}$$

$$\sigma^2_{\text{AD}} = \frac{1}{N-1} \sum_{i=1}^{N-1} \frac{(a_i - a_{i+1})^2}{a_i^2 + a_{i+1}^2} \tag{13}$$

### 2.2 Swept Source Optical Coherence Tomography

Optical coherence tomography angiography was performed using an ultrahigh speed Swept Source-OCT (SS-OCT) research prototype developed at the Mas-

**Table 1.** Results of the observer study. The grading ranges from 1 (very good) to 5 (very bad).

| | SV-OCTA | IFV-OCTA | AD-OCTA |
|---|---|---|---|
| Grade ($\mu \pm \sigma$) | $2.2 \pm 1.22$ | $2.24 \pm 1.13$ | $3.16 \pm 1.07$ |

sachusetts Institute of Technology and in use at the New England Eye Center. A similar OCT system was described previously and therefore only key characteristics are summarized herein [4]. The prototype OCT instrument uses a vertical cavity surface emitting laser (VCSEL) swept light source with a 400 kHz A-scan rate. The light source is centered at $1,050$ nm wavelengths. Optical coherence tomography interferometric signals were acquired with an analog-to-digital acquisition card externally clocked at a maximum frequency of $\sim 1.1$ GHz using an external Mach-Zehnder interferometer. Optical coherence tomography angiography imaging was performed with $6\,\text{mm} \cdot 6\,\text{mm}$ and $3\,\text{mm} \cdot 3\,\text{mm}$ fields of view. For both field sizes, 5 repeated B-scans from 500 uniformly spaced locations were sequentially acquired. Each B-scan consisted of 500 A-scans, which yields an isotropic transverse sampling. The fundamental interscan time between repeated B-scans was $\sim 1.5$ ms, accounting for the mirror scanning duty cycle. The acquisition time for repeated B-scans was $\sim 7.5$ ms ($5 \cdot 1.5$ ms) per position. A total of $5 \cdot 500 \cdot 500$ A-scans were acquired per OCTA volume for a total acquisition time of $\sim 3.9$ s.

### 2.3 Observer Study

Retrospective data of 5 subjects was used for this study, which were scanned at the New England Eye Center. The OCTA signal was computed with the SV-OCTA, IFV-OCTA and AD-OCTA formulas. The volumes were post processed with a volumetric median filter with radius 1. For the SV-OCTA and IFV-OCTA methods, the volumes were additionally logarithmized to optimize the intensity distribution. This step was not necessary for the AD-OCTA volume due to the intrinsic normalization. The observers were allowed to adjust the displayed intensity window. The volumetric data was viewed directly, no projection along depth was performed. 5 experts graded the vessel visibility of each volume on a scale from 1 (very good) to 5 (very bad).

## 3 Results

Fig. 1 shows the three OCTA measures computed at the same depth through a dataset of a healthy subject. The results of the observer study suggest that the IFV-OCTA measure is on par with the established measures (Table 1).

**Fig. 1.** Representative slices at the same depth in the SV-OCTA, IFV-OCTA and AD-OCTA volumes. All volumes were post processed with a median filter with radius 1. The SV-OCTA and IFV-OCTA volumes were additionally logarithmized.

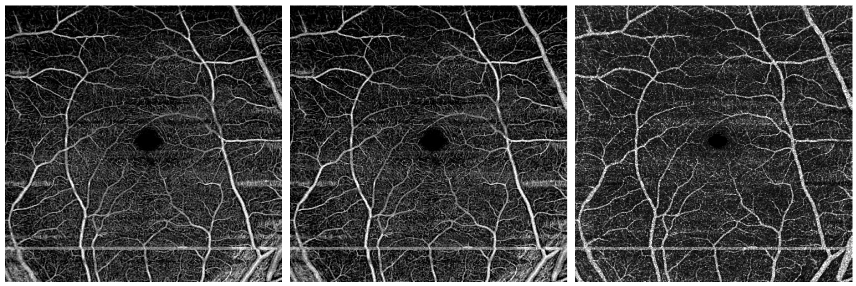

(a) SV-OCTA (b) IFV-OCTA (c) AD-OCTA

## 4 Discussion

This work's contribution is twofold. First, a probabilistic model for AD-OCTA was formulated, which was found to be a normal distribution based on the amplitude-normalized intensity differences. This aids in the interpretation of AD-OCTA data because the inherent model assumptions are now apparent and can be compared to underlying physical principles. Furthermore, the model can be extended with denoising priors like, e.g., total variation, to incorporate denoising in the signal reconstruction step.

Second, the newly introduced IVF-OCTA computation formula can be seen as the missing link between SV-OCTA and AD-OCTA, which is especially apparent when comparing the objective functions. In a small sized study, the image quality of IFV-OCTA was comparable to the commonly used SV-OCTA and AD-OCTA methods. In the future, the IVF-OCTA method could be used in algorithms that require a dependency on the interscan time. An example for such a method is the VISTA algorithm [5,6], which was currently only applied to AD-OCTA data.

## References


1. Huang D, Swanson EA, Lin CP, et al. Optical Coherence Tomography. Science. 1991 11;254(5035):1178–1181.
2. Mariampillai A, Standish BA, Moriyama EH, et al. Speckle variance detection of microvasculature using swept-source optical coherence tomography. Opt Lett. 2008;33(13):1530.
3. Jia Y, Tan O, Tokayer J, et al. Split-spectrum amplitude-decorrelation angiography with optical coherence tomography. Opt Express. 2012;20(4):4710–4725.
4. Choi W, Potsaid B, Jayaraman V, Baumann B, et al. Phase-sensitive swept-source optical coherence tomography imaging of the human retina with a vertical cavity surface-emitting laser light source. Opt Lett. 2013;38(3):338–340.
5. Choi W, Moult EM, Waheed NK, et al. Ultrahigh-speed, swept-source optical coherence tomography angiography in nonexudative age-related macular degeneration with geographic atrophy. Ophthalmology. 2015;122(12):2532–2544.

6. Ploner SB, Moult EM, Choi W, et al. Toward Quantitative Optical Coherence Tomography Angiography: Visualizing Blood Flow Speeds in Ocular Pathology Using Variable Interscan Time Analysis. Retina. 2016;36 Suppl 1:S118–S126.